Antibody Therapeutics, 2022, Vol. 5, No. 3 ***151–163***
https://doi.org/10.1093/abt/tbac013
Advance Access Publication on 10 June 2022

Original research article

Intracellular flow cytometry staining of antibody-secreting cells using phycoerythrin-conjugated antibodies: pitfalls and solutions

Patrick Renner[1,†], Michael Crone[1,†], Matthew Kornas[1,†], KimAnh T. Pioli[1,2] and Peter D. Pioli[1,2,*]

[1]Department of Investigative Medicine, Western Michigan University Homer Stryker M.D. School of Medicine, Kalamazoo 49008, USA , and [2]Department of Biochemistry, Microbiology and Immunology, University of Saskatchewan, Saskatoon S7N 5E5, Canada

Received: April 4, 2022; Revised: June 2, 2022; Accepted: June 7, 2022

ABSTRACT

Background: Antibody-secreting cells are terminally differentiated B cells that play a critical role in humoral immunity through immunoglobulin secretion along with possessing the potential to be long-lived. It is now appreciated that ASCs regulate multiple aspects of biology through the secretion of various cytokines. In this regard, ICFC is a key tool used to assess the presence of intracellular proteins such as cytokines and transcription factors.
Methods: Paraformaldehyde plus saponin or the eBioscience Foxp3/Transcription Factor Staining Buffer Set were used to evaluate the non-specific intracellular retention of phycoerythrin-containing antibody conjugates by ASCs.
Results: We showed that the use of phycoerythrin-containing antibody conjugates led to a false interpretation of ASC intracellular protein expression compared with other cell types. This was mainly due to the inappropriate retention of these antibodies specifically within ASCs. Furthermore, we demonstrated how to reduce this retention which allowed for a more accurate comparison of intracellular protein expression between ASCs and other cell types such as B lymphocytes. Using this methodology, our data revealed that spleen ASCs expressed toll-like receptor 7 as well as the pro-form of the inflammatory cytokine interleukin-1β.
Conclusion: Increasing the number of centrifugation steps performed on ASCs post-fixation leads to inappropriate retention of phycoerythrin-containing antibody conjugates during ICFC.

Statement of Significance: Phycoerythrin (PE)-conjugated antibodies (Abs) are heavily used in intracellular flow cytometry due to their high signal-to-noise ratio. By reducing the number of post-fixation centrifugation steps, we reduce antibody-secreting cell (ASC) non-specific retention of PE-conjugated Abs. This opens the door to reliably using these reagents to assess ASC intracellular proteins.

KEYWORDS: antibody-secreting cell; plasma cell; plasmablast; phycoerythrin; intracellular flow cytometry

INTRODUCTION

Humoral, or antibody (Ab)-mediated, immunity plays a critical role in host defense [1]. Through a variety of mechanisms, the activation of B cells can lead to their terminal differentiation into antibody-secreting cells (ASCs) which include relatively short-lived plasmablasts

*To whom correspondence should be addresses. Peter D. Pioli. Email: peter.pioli@usask.ca.
†These authors share first authorship.

(PBs) as well as more mature plasma cells (PCs) [2–5]. In general, ASCs are viewed as critical effectors of humoral immunity through their potential to be long-lived [6, 7] as well as their continuous production of Abs [8]. It is appreciated that ASCs influence host biology beyond the direct effects of Ab synthesis [9–11]. Given that ASCs are programmed for protein production and secretion [12, 13], it is not a surprise that many of the functions they exert are mediated by cytokine production. For example, ASCs utilize interleukin (IL)-10 to suppress the inflammatory response in the context of autoimmunity [14, 15]. However, ASCs can also facilitate the immune response through the production of factors including IL-6 [16] as well as IL-3 [17] and granulocyte-macrophage colony-stimulating factor (GM-CSF) [18, 19].

Multiple strategies currently exist which allow for the evaluation of ASC cytokine production. For instance, ASCs can be isolated via fluorescence-activated cell sorting (FACS), stimulated *in vitro* and cultured supernatants directly probed for selected cytokines [20]. While informative, this approach requires knowing the correct stimulus or stimuli and does not necessarily provide insight into the cytokines that ASCs are actively producing while residing within a particular tissue. As such, this type of analysis has been paired with *in vivo* techniques that utilize fluorescent reporter mice such as those specific for IL-10 [14, 20–23]. However, since genetically engineered reporter mice are not readily available for most cytokines, intracellular flow cytometry (ICFC) is also extensively performed to assess ASC cytokine production [17–19]. Indeed, this approach was recently used to show that PBs produced IL-3 and GM-CSF in the context of malaria-inducing parasitic infections [17].

Within the field of flow cytometry, phycoerythrin (PE)-conjugated Abs are known to be extremely "bright" and provide large signal-to-noise ratios thus facilitating their use to detect rare protein targets [24]. However, a previous study has shown that ASCs nonspecifically retain PE during ICFC [25]. This artifact pertains to *ex vivo* stained ASCs as well as those derived *in vitro*. Additionally, nonspecific PE retention was observed when ICFC was performed on day 3 cultures from lipopolysaccharide (LPS)-stimulated B cells [26], a time point known to generate a significant proportion of ASCs. Thus, this retention phenomenon is a confounding factor in the analysis of ASC cytokine production and evaluation with ICFC.

In this study, we showed that the complication of nonspecific PE retention by ASCs also pertained to PE-containing tandem fluorochromes such as PE/Cy7. The number of centrifugation steps postfixation directly modulated the extent of this retention. Provided here is a standard approach that reduces PE retention allowing for the use of PE- and PE/Cy7-conjugates Abs to perform ICFC on ASCs. Via this methodology, we demonstrated that spleen (SPL) PBs and PCs stained positive for Pro-IL-1β. Furthermore, we detected TLR7 protein expression by PBs and PCs thus adding to the growing list of immunomodulatory receptors that these cells possess.

MATERIALS AND METHODS

Mice

B6.Cg-Tg(Prdm1-EYFP)1Mnz/J (Stock #: 008828) and wild-type C57BL/6 mice were purchased from the Jackson Laboratory and used to establish a breeding colony within the vivarium of the Western Michigan University Homer Stryker M.D. School of Medicine (WMed). Genetically wild-type (i.e., lacking the Prdm1-eYFP transgene) mice were used for all experiments. Prdm1-eYFP expressing mice were used for a separate project. Both females and males were used between 12 and 32 weeks of age for experiments in Figs 1–4 and Supplementary Figs 1–3. However, 25-weeks-old males were specifically used in Fig. 5 and Supplementary Fig. 4 to correct for any potential age- or sex-based effects on target protein expression.

Isolation of spleen tissue

SPLs were collected in calcium and magnesium-free 1x phosphate-buffered saline (PBS). Organs were crushed between the frosted ends of two slides and cell suspensions were centrifuged for 5 minutes at 4 °C and 600 g. Red blood cells were lysed by resuspending (RSS) cells in 3 mL of 1x red blood cell lysis buffer on ice for ~3 minutes. Lysis was stopped with the addition of 7 mL of 1x PBS. Cell suspensions were counted via a hemocytometer using trypan blue to exclude dead cells and subsequently passed through 70 μm filters, centrifuged as discussed earlier and RSS in 1x PBS + 0.1% bovine serum albumin (BSA) at a concentration of 2×10^7 cells/mL.

Cell surface immunostaining for flow cytometry

Cell surface staining procedures were performed in 1x PBS + 0.1% BSA using $\sim 5 \times 10^6$ cells per stain. Samples were labeled with a CD16/32 blocking Ab to eliminate the nonspecific binding of Abs to cells via Fc receptors. All Abs utilized are listed in Supplementary Table 1. Cells were incubated on ice for 30 minutes with the appropriate Abs. Unbound Abs were removed with 3 mL of 1x PBS + 0.1% BSA followed by centrifugation for 5 minutes at 4 °C and 600 g. Supernatants were decanted. In certain instances, eBioscience Fixable Viability (Live-Dead) Dye eFluor 780 (Thermo Fisher Scientific, Catalog # 65–0865-14) was added to samples to assess dead cell content. The stock solution was diluted at 1:250 and 10 μL was added to $\sim 5 \times 10^6$ cells per stain. The live-dead stain was added concurrently with surface staining Abs.

Paraformaldehyde and saponin immunostaining for ICFC

Cells were surface stained as described earlier. Afterward, cell pellets were RSS in 1 mL of 4% paraformaldehyde (PFA) and incubated at room temperature (RT) for 20 minutes in the dark. Subsequently, 2 mL of 1x PBS + 0.1% BSA + 0.1% Saponin (Sap) were added and cells centrifuged for 5 minutes at 4 °C and 600 g. Supernatants were decanted and the previous step was repeated with

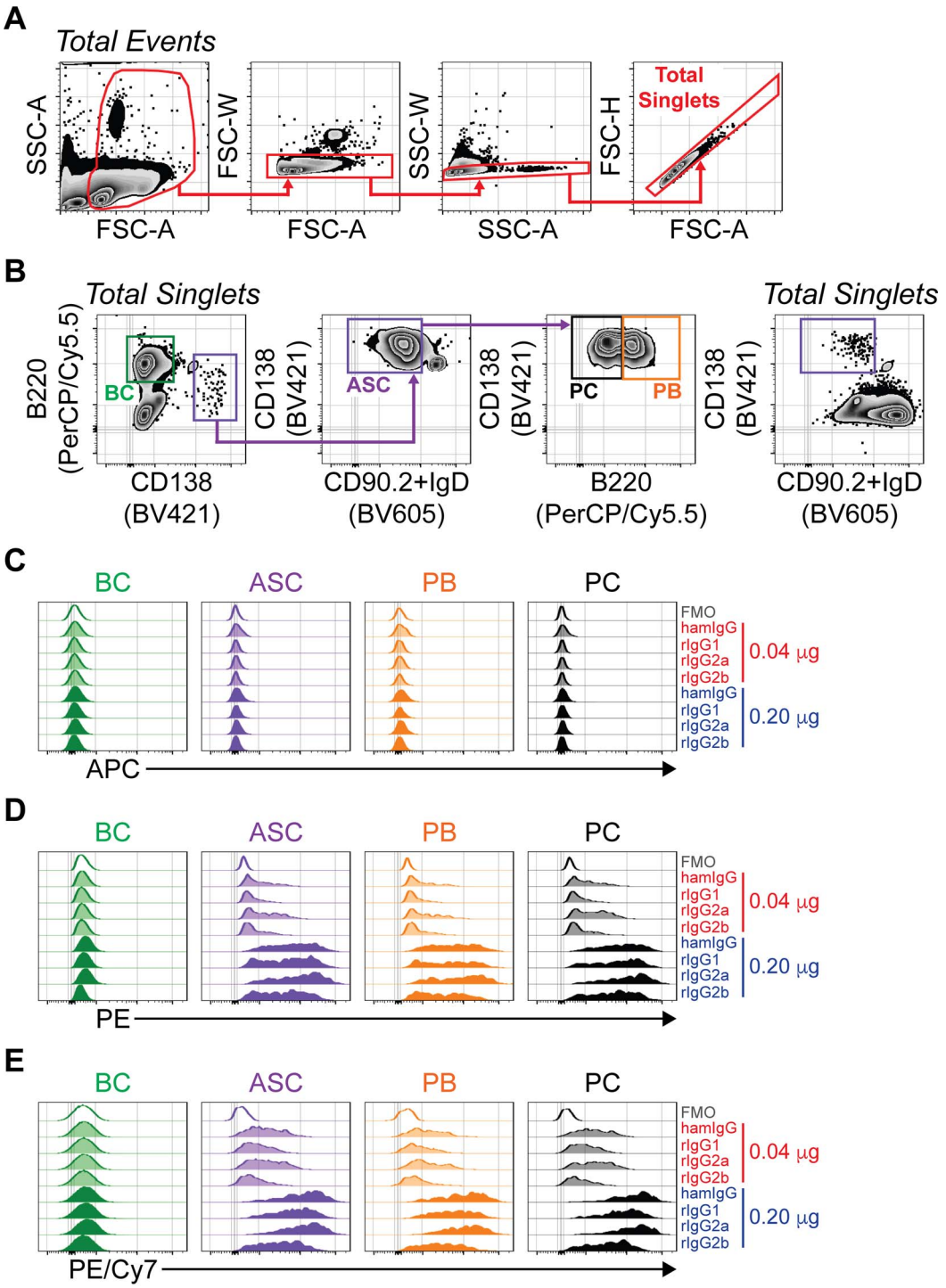

Figure 1. ASCs nonspecifically retain PE- and PE/Cy7-conjugated Abs. (**A**) Representative flow cytometry plots demonstrating gating of total singlets. (**B**) Representative flow cytometry plots demonstrating gating of SPL $B220^{+}$ $CD138^{-}$ BCs and $B220^{+/-}$ $CD138^{HI}$ $CD90.2^{-}$ IgD^{-} ASCs. Total ASCs are further subdivided into $B220^{+}$ PB and $B220^{-}$ PC. Cells are pregated on total singlets. CD138 versus CD90.2 + IgD staining of total singlets is shown for reference. (**C**–**E**) Flow cytometry overlay histograms showing fluorescence intensity for (C) APC, (D) PE, and (E) PE/Cy7. FMO and isotype control Ab (0.04 and 0.020 μg) stains are shown for SPL BCs, total ASCs, PBs, and PCs. Data are representative of three individual experiments and gMFIs are summarized in Supplementary Fig. 1.

3 mL of 1x PBS + 0.1% BSA + 0.1% Sap for a total of two centrifugations. The supernatants were discarded and cells were RSS in residual buffer (~150 μL). Unlabeled mouse IgG was added as a blocking reagent and cells were incubated at RT for 20 minutes in the dark. Subsequently, the appropriate Abs were added and cells were incubated at RT for 30 minutes in the dark. Afterward, 3 mL of 1x PBS + 0.1% BSA + 0.1% Sap were added and cells

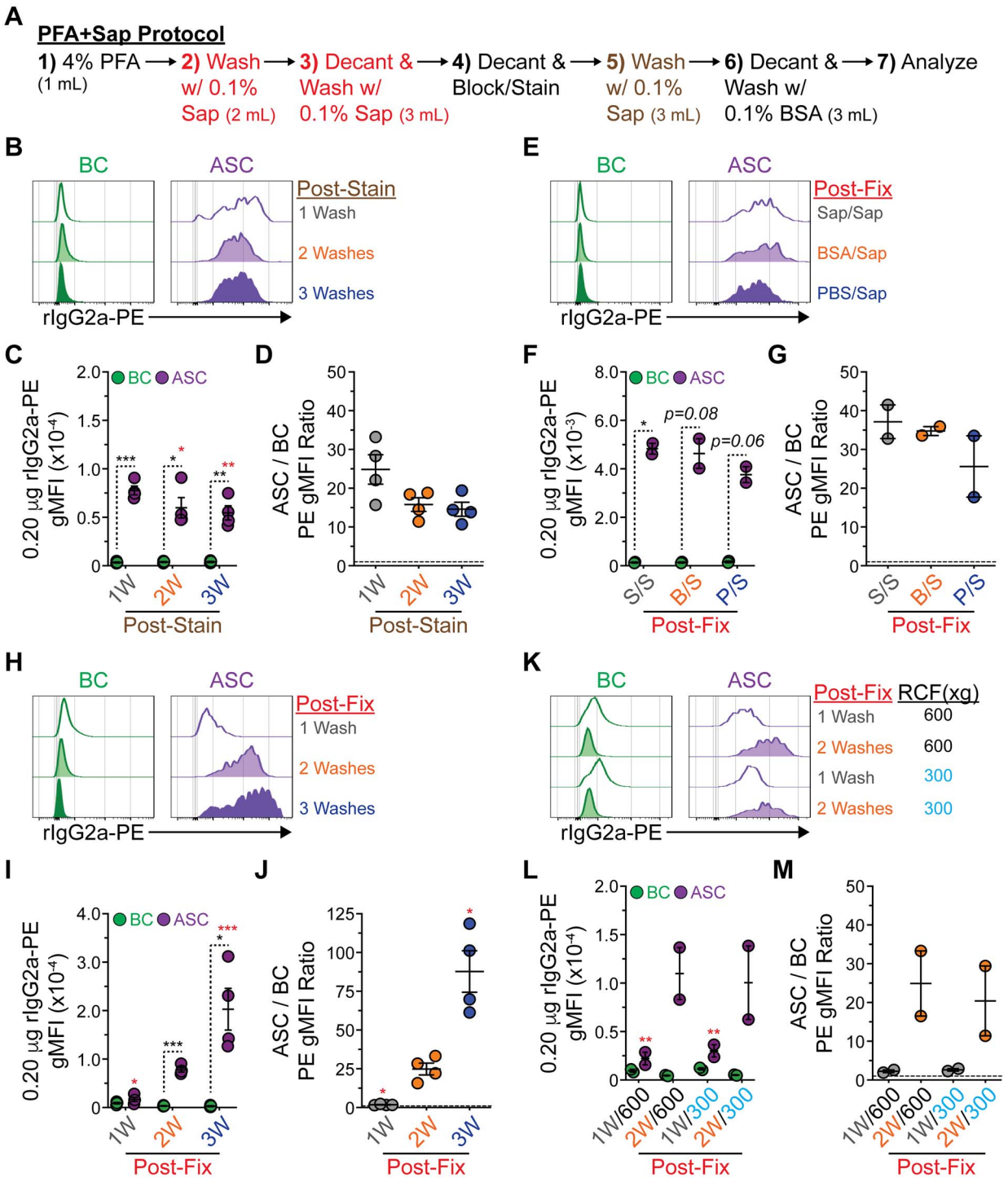

Figure 2. The number of postfixation washes modulates ASC retention of PE- and PE/Cy7-conjugated Abs. (**A**) Schematic depicting PFA + Sap staining protocol. (**B**) Flow cytometry overlay histograms showing rIgG2a-PE fluorescence intensity for SPL BCs and ASCs using 1, 2, or 3 poststain Sap washes. (**C**) rIgG2a-PE (0.20 μg) gMFIs of SPL BCs and ASCs washed 1, 2, or 3 times with Sap following staining. (**D**) Ratio of SPL ASC/BC rIgG2a-PE (0.20 μg) gMFIs from cells washed 1, 2, or 3 times with Sap following staining. Horizontal dashed line represents a ratio of 1. (**E**) Flow cytometry overlay histograms showing rIgG2a-PE fluorescence intensity for SPL BCs and ASCs using Sap/Sap, BSA/Sap or PBS/Sap two-step washes postfixation. (**F**) rIgG2a-PE (0.20 μg) gMFIs of SPL BCs and ASCs washed with Sap/Sap (S/S), BSA/Sap (B/S) or PBS/Sap (P/S). (**G**) Ratio of SPL ASC/BC rIgG2a-PE (0.20 μg) gMFIs from cells washed with S/S, B/S, or P/S. Horizontal dashed line represents a ratio of 1. (**H**) Flow cytometry overlay histograms showing rIgG2a-PE fluorescence intensity for SPL BCs and ASCs using 1, 2, or 3 postfixation Sap washes. (**I**) rIgG2a-PE (0.20 μg) gMFIs of SPL BCs and ASCs washed 1, 2, or 3 times with Sap following fixation. (**J**) Ratio of SPL ASC/BC rIgG2a-PE (0.20 μg) gMFIs from cells washed 1, 2, or 3 times with Sap following fixation. Horizontal dashed line represents a ratio of 1. (**K**) Flow cytometry overlay histograms showing rIgG2a-PE fluorescence intensity for SPL BCs and ASCs using one or two postfixation Sap washes at 600 or 300 g. (**L**) rIgG2a-PE (0.20 μg) gMFIs of SPL BCs and ASCs washed 1 or 2 times at 600 or 300 g with Sap following fixation. **(M)** Ratio of SPL ASC/BC rIgG2a-PE (0.20 μg) gMFIs from cells washed 1 or 2 times at 600 or 300 g with Sap following fixation. Horizontal dashed line represents a ratio of 1**. (B–D, H–J)** Data derived from four separate experiments. (**E–G, K–M**) Data

centrifuged for 5 minutes at 4 °C and 600 g. The supernatants were decanted and cells were centrifuged again in the presence of 3 mL of 1x PBS + 0.1% BSA. The supernatants were discarded and cell pellets were RSS in an appropriate volume of 1x PBS + 0.4% BSA + 2 mM ethylenediaminetetraacetic acid (EDTA) for flow cytometry. Before analysis, cells were strained through a 35 μM filter mesh. Deviations from centrifugation step constituents or sequence are noted in the Results section.

Methanol immunostaining for ICFC

Cells were surface stained as described earlier. Afterward, cell pellets were RSS in 1 mL of ice-cold 100% methanol (MeOH) and incubated on ice for 20 minutes in the dark. Subsequently, 2 mL of 1x PBS + 0.1% BSA were added and cells were centrifuged for 5 minutes at 4 °C and 600 g. Supernatants were decanted and the previous step was repeated with 3 mL of 1x PBS + 0.1% BSA for a total of two centrifugations. The supernatants were discarded and cells were RSS in residual buffer (~150 μL). Unlabeled mouse IgG was added as a blocking reagent and cells were incubated at RT for 20 minutes in the dark. Subsequently, the appropriate Abs were added and cells were incubated at RT for 30 minutes in the dark. Afterward, 3 mL of 1x PBS + 0.1% BSA were added and cells were centrifuged for 5 minutes at 4 °C and 600 g. The supernatants were decanted and cells were centrifuged again in the presence of 3 mL of 1x PBS + 0.1% BSA. The supernatants were discarded and cell pellets were RSS in an appropriate volume of 1x PBS + 0.4% BSA + 2 mM EDTA for flow cytometry. Before analysis, cells were strained through a 35 μM filter mesh.

eBioscience Foxp3/transcription factor staining buffer set immunostaining for ICFC

For this procedure, ICFC was performed with the eBioscience Foxp3/Transcription Factor Staining Buffer Set (Thermo Fisher Scientific, Catalog # 00–5523-00). Cells were surface stained as described earlier. Afterward, cell pellets were RSS in 1 mL of Buffer 1 and incubated at RT for 20 minutes in the dark. Subsequently, 2 mL of Buffer 2 was added and cells were centrifuged for 5 minutes at 4 °C and 600 g. Supernatants were decanted and the previous centrifugation step was repeated with 2 mL of Buffer 2 for a total of 2 centrifugations. Supernatants were discarded and cells were RSS in residual buffer (~150 μL). Unlabeled mouse IgG was added as a blocking reagent and cells were incubated at RT for 20 minutes in the dark. Subsequently, the appropriate Abs were added and cells were incubated at RT for 30 minutes in the dark. Afterward, 2 mL of Buffer 2 was added and cells were centrifuged for 5 minutes at 4 °C and 600 g. Supernatants were decanted and cells were centrifuged again in the presence of 3 mL of 1x PBS + 0.1% BSA. Supernatants were discarded and cell pellets were RSS in an appropriate volume of 1x PBS + 0.4% BSA + 2 mM EDTA for flow cytometric analysis. Before analysis, cells were strained through a 35 μM filter mesh. Deviations from centrifugation step constituents or sequence are noted in the Results section.

Flow cytometry

Flow cytometry was performed on a Fortessa (BD Biosciences) located in the Flow Cytometry and Imaging Core at WMed. This instrument is equipped with five lasers (355, 405, 488, 561 and 640 nm). The full configuration including lasers and corresponding detectors is included in Supplementary Table 2. Data were analyzed using FlowJo (v10) software. Total cells were gated using the side scatter area (SSC-A) versus forward scatter area (FSC-A). Singlets were identified using sequential gating of FSC-width (W) versus FSC-A, SSC-W versus SSC-A and FSC-height (H) versus FSC-A.

Fluorescence-activated cell sorting

Prior to sorting, prestained (surface and intracellular) SPL cells were resuspended at 2×10^7 cells/mL in 1x PBS + 0.4% BSA + 2 mM EDTA. Cells were sorted into ~ 150 μL of 1x PBS + 0.1% BSA using a FACSMelody (BD Biosciences) cell sorter located in the Flow Cytometry and Imaging Core at WMed. Sorting was performed using a similar gating strategy as shown in Fig. 1.

Immunofluorescence imaging

Prior to imaging, FACS-purified SPL B cells (BCs) and ASCs were cytospun onto Superfrost Plus microscope slides using a Thermo Scientific Cytospin 4. Coverslips were mounted using SlowFade Diamond Antifade Mountant (Thermo Fisher Scientific, Catalog # S36963). Slides were imaged using an EVOS M7000 Imaging System with a 40X objective (Thermo Fisher Scientific, Catalog # AMF7000).

Quantification and statistical analysis

Technical and biological replicates are indicated in the figure legends. Statistics were performed using GraphPad Prism 9. Paired two-way analysis of variance (ANOVA) with Sidak's (Fig. 4, Supplementary Figs. 1 and 3), Dunnett's (Figs. 2–3 and 5, Supplementary Figs. 1 and 4), or Tukey's (Fig. 5) multiple comparisons test, paired one-way

derived from two separate experiments. (**C, D, F, G, I, J, L, M**) Symbols represent individual mice. Horizontal lines represent mean ± SEM. (C, F, I, L) Comparisons between BC and ASC: Paired Student *t*-test. *P*-values: $^*P < 0.05$, $^{**}P < 0.01$ and $^{***}P < 0.001$. Mixed cell type and wash comparisons (e.g., BC 1 W versus ASC 3 W) were omitted for simplicity. Comparisons within cell type: paired two-way ANOVA with Dunnett's multiple comparisons test. Controls set as (C) 1 W, (F) S/S, (I) 2 W, and (L) 2 W/600. Red asterisks denote significance compared with controls. *P*-values: $^*P < 0.05$, $^{**}P < 0.01$, $^{***}P < 0.001$, and $^{****}P < 0.0001$. (D, G, J, M) Paired one-way ANOVA with Dunnett's multiple comparisons test. Controls set as (D) 1 W, (G) S/S, (J) 2 W, and (M) 2 W/600. Red asterisks denote significance compared with controls. *P*-value: $^*P < 0.05$.

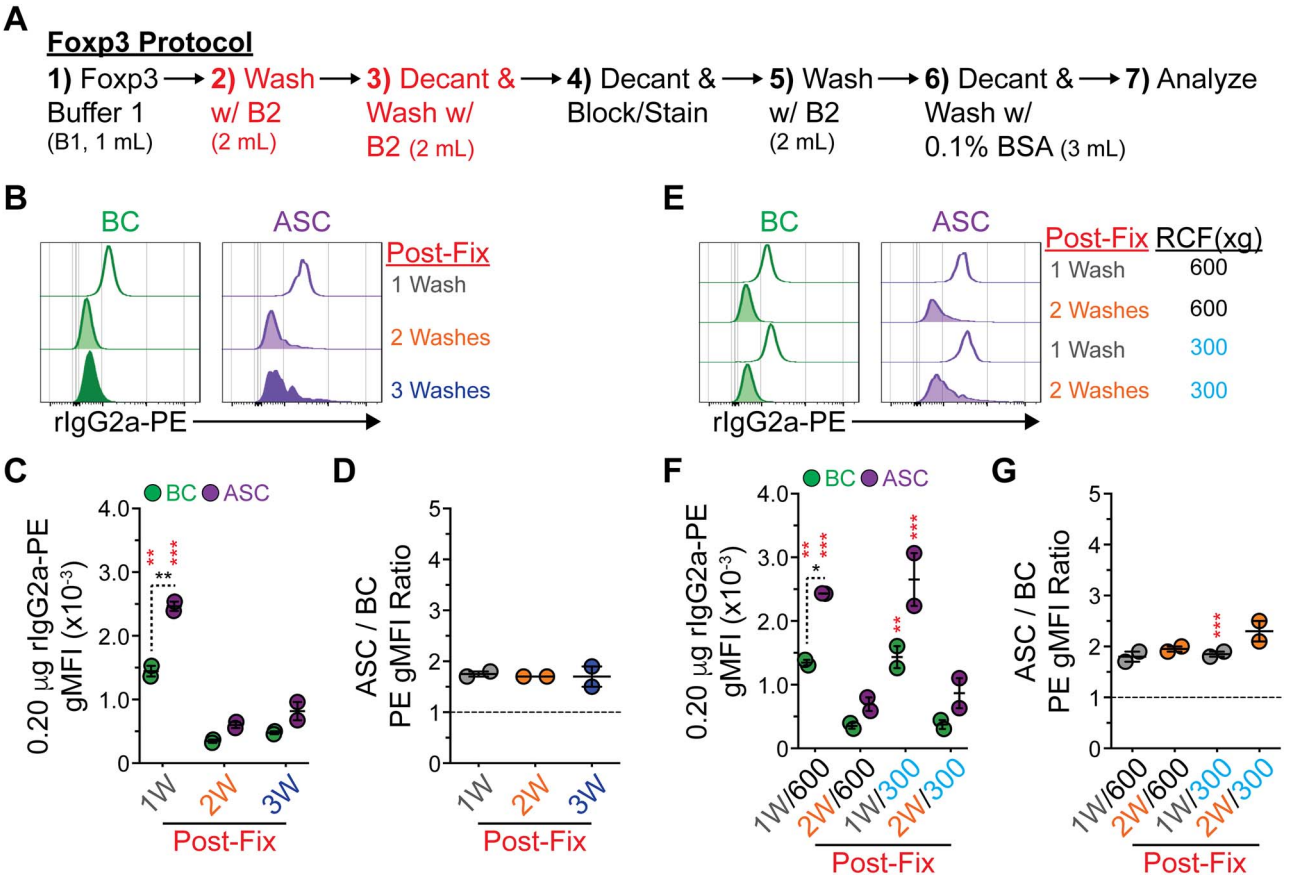

Figure 3. The number of postfixation washes modulates ASC retention of PE-conjugated Abs when using the eBioscience Foxp3/Transcription Factor Staining Buffer Set. (**A**) Schematic depicting Foxp3 staining protocol. (**B**) Flow cytometry overlay histograms showing rIgG2a-PE fluorescence intensity for SPL BCs and ASCs using one, two or three postfixation Foxp3 B2 washes. (**C**) rIgG2a-PE (0.20 μg) gMFIs of SPL BCs and ASCs washed 1, 2, or 3 times with Foxp3 B2 following fixation. (**D**) Ratio of SPL ASC/BC rIgG2a-PE (0.20 μg) gMFIs from cells washed 1, 2, or 3 times with Foxp3 B2 following fixation. Horizontal dashed line represents a ratio of 1. (**E**) Flow cytometry overlay histograms showing rIgG2a-PE fluorescence intensity for SPL BCs and ASCs using one or two postfixation Foxp3 B2 washes at 600 or 300 g. (**F**) rIgG2a-PE (0.20 μg) gMFIs of SPL BCs and ASCs washed 1 or 2 times at 600 or 300 g with Foxp3 B2 following fixation. (**G**) Ratio of SPL ASC/BC rIgG2a-PE (0.20 μg) gMFIs from cells washed 1 or 2 times at 600 or 300 g with Foxp3 B2 following fixation. Horizontal dashed line represents a ratio of 1. (B–G) Data derived from two separate experiments. (C, D, F, G) Symbols represent individual mice. Horizontal lines represent mean ± SEM. (C, F) Comparisons between BC and ASC: paired Student *t*-test. *P*-values: $^{*}P < 0.05$, $^{**}P < 0.01$. Mixed cell type and wash comparisons (e.g., BC 1 W versus ASC 3 W) were omitted for simplicity. Comparisons within cell type: paired two-way ANOVA with Dunnett's multiple comparisons test. Controls set as (C) 2 W and (F) 2 W/600. Red asterisks denote significance compared with controls. *P*-values: $^{**}P < 0.01$ and $^{***}P < 0.001$. (D, G) Paired one-way ANOVA with Dunnett's multiple comparisons test. Controls set as (D) 2 W and (G) 2 W/600. Red asterisks denote significance compared with controls. *P*-value: $^{***}P < 0.001$.

ANOVA with Tukey's (Supplementary Figs. 3–4) or Dunnett's (Figs. 2–3) multiple comparisons test and paired Student *t*-tests (Figs. 2–3, Supplementary Fig. 4) were utilized as indicated in the figure legends. Statistically significant *P*-values are noted in the figure legends as $^{*}P < 0.05$, $^{**}P < 0.01$, $^{***}P < 0.001$ and $^{****}P < 0.0001$.

RESULTS

ASCs preferentially retain PE-conjugated antibodies

ICFC of cytokines has become a critical tool used to evaluate ASC diversification and function. Using conventional fixation (i.e., PFA) and permeabilization (i.e., Sap) techniques, it has been reported that ASCs nonspecifically retain PE-conjugated Abs thus making them unsuitable for ICFC [25]. This was shown to be the case for *ex vivo* stained ASCs as well as those generated *in vitro* following B lymphocyte stimulation [25].

To better characterize this phenomenon, we evaluated the ability of ASCs from the SPL to retain a variety of nonspecific isotype control Abs conjugated to allophycocyanin (APC), PE and PE/Cy7. Total singlets were sequentially gated as shown in Fig. 1A. ASCs were subsequently identified as B220$^{+/-}$ CD138^{HI} CD90.2^{-} IgD^{-} (Fig. 1B). As ASCs in the SPL do not normally express IgD (a naïve B cell marker) or CD90.2 (a pan T cell marker), these surface antigens were combined into a single channel to increase the accuracy of ASC gating. As a point of comparison, we also examined the retention capacity of SPL B220^{+} CD138^{-} BCs (Fig. 1B). For these experiments, we utilized hamster (ham) IgG, rat (r) IgG1, rIgG2a and rIgG2b isotypes. Using flow cytometry, retention was measured as a function of geometric mean fluorescence intensity (gMFI). In

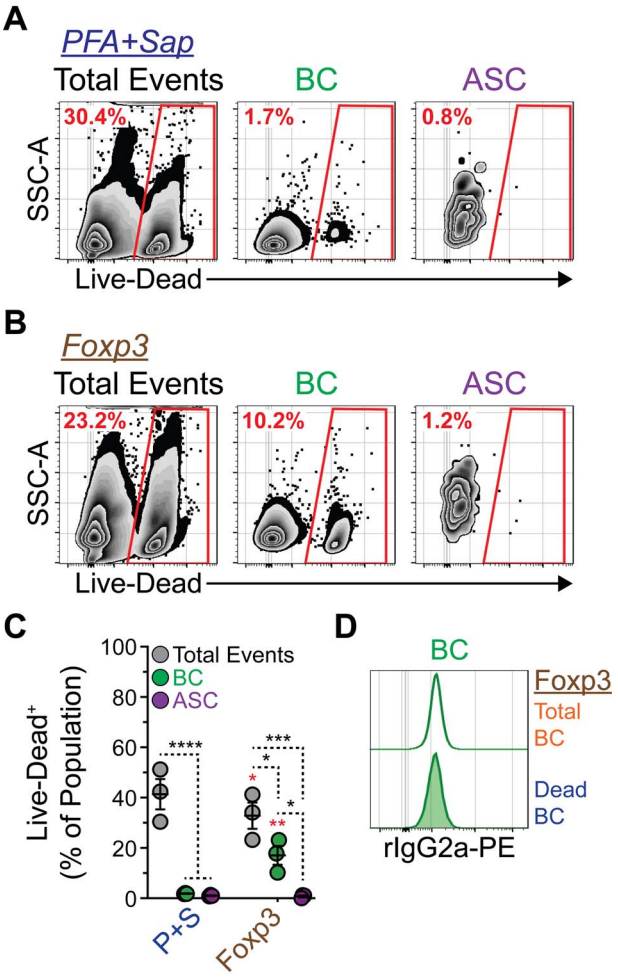

Figure 4. Fixation and permeabilization method does not differentially impact the analysis of live versus dead ASCs. (**A, B**) Representative flow cytometry plots demonstrating live-dead staining of total SPL events as well as gated BCs and ASCs. Samples were processed using (A) PFA + Sap or the (B) Foxp3 buffer set. Dead cells are gated and percentages of live-dead$^+$ cells are indicated in red. (**C**) Percentages of live-dead$^+$ cells within total SPL events, BCs and ASCs. Symbols represent individual mice. Horizontal lines represent mean ± SEM. Paired two-way ANOVA with Sidak's multiple comparisons test. *P*-values: $^*P < 0.05$, $^{**}P < 0.01$, $^{***}P < 0.001$, and $^{****}P < 0.0001$. Red asterisks indicate comparisons between P + S versus Foxp3 within a given cell type. Mixed cell type and buffer comparisons (e.g., P + S total events versus Foxp3 ASC) were omitted for simplicity. (**D**) Flow cytometry overlay histograms showing rIgG2a-PE fluorescence intensity for total and dead SPL BCs using the Foxp3 buffer set. (A–D) Data are derived from two separate experiments.

this regard, increased isotype Ab gMFIs as compared with fluorescence minus one (FMO) controls were indicative of increased retention (Supplementary Fig. 1A–F).

In general, Abs conjugated to APC produced very little background when compared with FMO controls (Fig. 1C and Supplementary Fig. 1A). This was independent of Ab amount and observed in both BCs and ASCs. However, the examination of PE-conjugated isotype Abs painted a different picture. While BC and ASC FMO controls possessed similar amounts of PE-mediated background autofluorescence (Fig. 1D and Supplementary Fig. 1C), the use of low amounts (0.04 μg) of PE-conjugated isotype Abs resulted in low levels of retention in ASCs relative to BCs (Fig. 1D and Supplementary Fig. 1C), whereas increased Ab amounts (0.20 μg) led to further retention by ASCs which was apparent for all isotypes (Fig. 1D and Supplementary Fig. 1C). To determine if these observations could be more generalized, we examined the retention of the tandem dye PE/Cy7 (Fig. 1E and Supplementary Fig. 1E). Similar to PE, PE/Cy7 retention by ASCs was evident in an Ab amount-dependent manner regardless of isotype (Fig. 1E and Supplementary Fig. 1E).

Additionally, we subdivided ASCs (Fig. 1B) into short-lived PBs and more mature, potentially long-lived PCs which are B220$^+$ and B220$^-$, respectively. Analysis of APC-, PE- and PE/Cy7-conjugated isotype Ab retention demonstrated a high degree of similarity between PBs and PCs (Fig. 1C–E and Supplementary Fig. 1B, D and F). These data indicated that the maturation status of ASCs (PBs vs. PCs) did not explicitly alter the capacity to retain PE- and PE/Cy7-conjugated isotype Abs. Furthermore, these results suggested that potential contamination with non-ASCs that possess B220 expression (e.g., plasmacytoid dendritic cells (pDCs)) did not influence the data. In summary, ASCs displayed retention of PE-based fluorochromes that was independent of Ab isotype and species but was augmented by increased Ab amounts. These data were consistent with previous findings demonstrating PE retention in the absence of Ab conjugation [25, 26].

Phycoerythrin retention in ASCs presents as a punctate staining pattern

Immunofluorescence (IF) microscopy of B cell cultures 3 days post-LPS stimulation demonstrated a punctate staining pattern of PE retention [26]. To confirm this observation, we performed ICFC on SPL cells using rIgG2a-PE (0.20 μg). BCs and ASCs were subsequently FACS-purified, cytospun and then imaged to evaluate the localization of PE retention (Supplementary Fig. 2). As expected, ASCs expressed CD138 as well as intracellular IgM (Supplementary Fig. 2). In contrast, BCs lacked a CD138 signal and IgM was largely restricted to the cell surface (Supplementary Fig. 2). Evaluation of rIgG2a-PE demonstrated a low level intracellular "haze," or background, for both cell types. However, ASCs possessed an additional punctate staining pattern that was absent in BCs (Supplementary Fig. 2) as confirmed in previous studies.

Fixative, wash buffer constitution and the number of post-stain washes are not responsible for the retention of phycoerythrin-conjugated antibodies by ASCs

For the purposes of this study, we use the term "wash" to refer to the centrifugation of cells in the presence of a particular buffer. In our staining protocol, we utilized one post-stain wash that included Sap (Fig. 2A, **brown**). This was then repeated with PBS + 0.1% BSA. Therefore, it is possible that additional Sap washes could abrogate PE retention. To test this, we performed experiments in which cells stained with rIgG2a-PE (0.20 μg) received 1, 2, or 3 post-stain Sap washes followed by a terminal

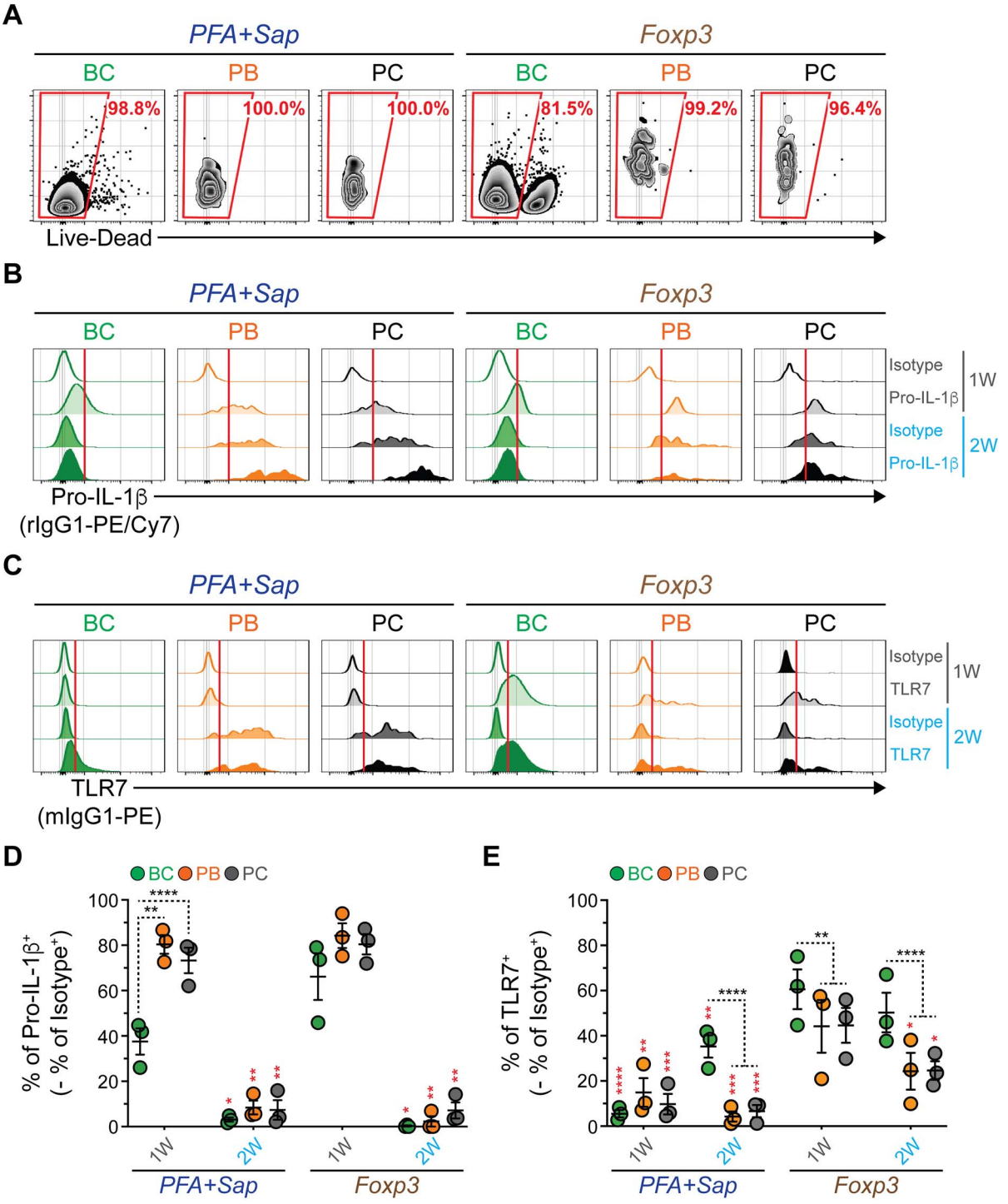

Figure 5. Performance of one postfixation wash using the eBioscience Foxp3/Transcription Factor Staining Buffer Set allows for robust intracellular staining of ASC proteins. (**A**) Flow cytometry plots showing live-dead staining of SPL CD19$^+$ BCs, PBs and PCs with one postfixation wash using PFA + Sap or Foxp3 protocols. Percentages indicate live cells gated within the indicated parent population. Results were similar for two postfixation washes. (**B**) Flow cytometry overlay histograms showing rIgG1-PE/Cy7 isotype control and Pro-IL-1β-PE/Cy7 fluorescence intensity for SPL CD19$^+$ BCs, PBs, and PCs with one or two postfixation washes using either PFA + Sap or Foxp3 protocols. (**C**) Flow cytometry overlay histograms showing mouse IgG1 (mIgG1)-PE isotype control and TLR7-PE fluorescence intensity for SPL CD19$^+$ BCs, PBs, and PCs with one or two postfixation washes using either PFA + Sap or Foxp3 protocols. (**B, C**) Red vertical lines added to histograms to depict positive staining for Pro-IL-1β and TLR7. (**D, E**) Percentages of (D) Pro-IL-1β^+ cells and (E) TLR7$^+$ cells within CD19$^+$ BCs, PBs, and PCs. Symbols represent individual mice. Horizontal lines represent mean ± SEM. Comparisons between BC, PB, and PC: Paired two-way ANOVA with Tukey's multiple comparisons test. *P*-values: $^{**}P < 0.01$ and $^{****}P < 0.0001$. Mixed wash and buffer comparisons (e.g., P + S 1 W versus Foxp3 2 W) were omitted for simplicity. Comparisons within cell type: paired two-way ANOVA with Dunnett's multiple comparisons test. Controls set as 1 W Foxp3. Red asterisks denote significance compared with controls. *P*-values: $^{*}P < 0.05$, $^{**}P < 0.01$, $^{***}P < 0.001$, and $^{****}P < 0.0001$. (A–E) Data are representative of three individual experiments.

PBS + 0.1% BSA wash (Fig. 2B–D). The number of post-stain Sap washes had no effect on BC background PE staining (Fig. 2B and C). The addition of a 2nd or even 3rd wash led to a small reduction of PE retention by ASCs compared with cells that received a single wash (Fig. 2D). However, the ASC/BC PE gMFI ratio (Fig. 2D) ranged from ∼14 to 33 regardless of the number of post-stain Sap washes. These data confirmed previous observations from studies in which multiple post-stain washes containing permeabilizing agents were ineffectively used to remove PE retention by ASCs [25, 26].

The experiments presented in Fig. 1 utilized two post-fixation washes with 0.1% Sap as part of a PBS + 0.1% BSA solution (Fig. 2A, red). While it is commonly appreciated that the fixation method can alter the immunostaining properties of cells [27], it is not readily known how the steps used to remove a fixative can alter immunostaining. To test this, we kept the 2nd postfixation wash constant and performed the 1st wash with PBS + 0.1% BSA + 0.1% Sap (Sap/Sap), PBS + 0.1% BSA (BSA/Sap), or PBS (PBS/Sap). Subsequently, we analyzed the retention of rIgG2a-PE (0.20 μg) by BCs and ASCs (Fig. 2E). Regardless of 1st wash composition, ASCs still retained rIgG2a-PE as shown by heightened PE gMFIs when compared with BCs (Figs 2E and F). Ultimately, the rIgG2a-PE background was increased ∼30x in ASCs (Fig. 2G).

In the previous experiments, fixation was performed with PFA and permeabilization, as well as intracellular staining, was performed in the presence of Sap. To rule out the contribution of either of these compounds to the observed retention phenotype, we evaluated rIgG2a-APC, rIgG2a-PE and rIgG2a-PE/Cy7 (0.20 μg per Ab) staining following fixation/permeabilization with ice-cold 100% MeOH (Supplementary Fig. 3A–F). In this setting, all washes and Ab incubation steps were performed with PBS + 0.1% BSA to eliminate continued exposure to any potential denaturing agent. Inspection of flow cytometry histograms revealed clear retention of rIgG2a-PE and rIgG2a-PE/Cy7 (Supplementary Fig. 3B). In the context of APC, ASCs had slightly increased fluorescence relative to BCs in both FMO and rIgG2a samples with the latter reaching significance (Supplementary Fig. 3C). However, rIgG2a-PE and -PE/Cy7 stained ASCs clearly demonstrated increased gMFIs, albeit with a high degree of variability, when compared with cell-matched FMOs or their BC counterparts (Supplementary Fig. 3D and E). In this regard, the ASC/BC rIgG2a ratio was higher in every PE and PE/Cy7 sample when examined against APC (Supplementary Fig. 3F). These data provided evidence to exclude PFA and Sap as causative agents for the PE retention phenotype observed by ASCs.

The number of washes following paraformaldehyde fixation modulates ASC retention of phycoerythrin-conjugated antibodies

Since the fixative, the number of poststain Sap washes as well as the postfixation wash buffer composition did not appear to play a major role, we considered "physical" forces involved in ICFC that may augment ASC retention of PE. Compared with naïve B cells, ASCs are complex cells whose cytoplasm is dominated by an extensive endoplasmic reticulum (ER) and Golgi network [28]. As such, the act of centrifugation and the forces imparted on BCs and ASCs may be different and result in the ASC-specific retention of PE. Along these lines, variations in centrifugation protocols can have dramatic effects on recovery as well as the viability of mechanically sensitive cells [29, 30]. Based on the previous experiments, we would hypothesize for the effects to be enacted postfixation and pre-Ab staining. To test this hypothesis, we repeated the retention experiments discussed earlier using either 1, 2, or 3 postfixation washes with PBS + 0.1% BSA + 0.1% Sap (Fig. 2H). Increasing the number of washes slightly decreased the already low levels of rIgG2a-PE (0.20 μg) staining in BCs (Fig. 2H and I). In contrast, rIgG2a-PE retention by ASCs was enhanced as more washes (i.e., centrifugation steps) were performed (Fig. 2H and I). When compared with BCs, the rIgG2a-PE staining of ASCs was near equivalence at one wash. At two washes, the ratio of ASC/BC PE gMFI was ∼25 (Fig. 2J) similar to that shown in Fig. 2D. Finally, the addition of a third wash increased this ratio to >85, on average (Fig. 2J). To further assess the impact of "force" effects on PE retention, we performed experiments in which cells received either one or two postfixation washes using a relative centrifugal force (RCF) of 600 or 300 g (Fig. 2K). If total RCF was a determining factor, ASCs which received single or multiple 300 g centrifugation steps would display less retention than their 600 g counterparts. However, the level of PE retention observed in ASCs correlated with the number of centrifugation steps rather than the amount of RCF imparted on cells (Fig. 2K). This was apparent when we quantified the gMFI of PE retention (Fig. 2L) as well as the ratio of ASC/BC PE retention (Fig. 2M). In both instances, ASCs washed twice routinely demonstrated increased levels of PE staining regardless of RCF. In total, these results indicated that the physical act of centrifugation post-PFA fixation was the most critical driver in ASC PE retention.

The number of postfixation washes modulates ASC retention of phycoerythrin-conjugated antibodies when using the eBioscience Foxp3/transcription factor staining buffer set

The experiments using PFA + Sap (Fig. 2) demonstrated that the number of postfixation wash steps significantly impacted the retention of PE by ASCs. Previous studies demonstrated PE retention by ASCs using a variety of commercial buffer sets [26], but the impact of centrifugation number on Ab retention has not yet been addressed. As such, we examined the effects of centrifugation using the eBioscience Foxp3/Transcription Factor Staining Buffer Set (Fig. 3A) which was utilized in the aforementioned study [26].

When we varied the number of postfixation washes with Foxp3 Buffer 2 (B2) (Fig. 3A, **red**), we again observed differences in retention. BCs showed a reduction in background PE staining which was most evident when one and two washes were compared (Fig. 3B and C). Unlike with PFA + Sap, increasing the number of Foxp3 B2 washes did not enhance ASC retention of PE (Fig. 3B and C). Rather,

the use of multiple washes lowered the overall PE gMFI in ASCs (Fig. 3B and C) as demonstrated by a left shift of the primary peak of fluorescence intensity. However, the use of two or three washes induced a separate artifact of PE retention as indicated by the "tails" present in the rIgG2a-PE histograms of multi-washed ASCs (Fig. 3B). Overall, we did not observe a major deviation in the ASC/BC PE gMFI ratio when different numbers of washes were compared (Fig. 3D). To further characterize this phenomenon, we repeated experiments from Fig. 2 in which we varied postfixation wash number and RCF. As with PFA + Sap, the number of physical washes (i.e., centrifugations) had the largest impact on PE retention by ASCs (Fig. 3E–G). While the artifacts induced by the number of washes were specific to buffer sets, they shared the common theme of modulation by the number of postfixation washes.

Fixation and permeabilization method does not differentially impact the analysis of live versus dead ASCs

Experiments in Figs 2 and 3 indicated that different fixation and permeabilization methodologies induced distinct types of PE retention artifacts in ASCs. Since both protocols are known to impact cellular morphology in their own unique fashion, it is possible that this led to a false comparison of ASCs between the two methods. That is, a particular method may have included a significant proportion of dead ASCs which skewed the results. To exclude this possibility, we repeated the single postfixation wash PFA + Sap and Foxp3 ICFC protocols with the inclusion of a fixable live-dead stain (Fig. 4A–D). As expected, total ungated events demonstrated a clear positive population indicative of dead cells regardless of the buffer system used (Fig. 4A–C). When using PFA + Sap, the percentages of gated BCs and ASCs that were Live-Dead$^+$ were ∼1.8% and 1.0%, respectively (Fig. 4A–C). The use of the Foxp3 buffer set increased the percentage of dead BCs that were analyzed to ∼17% (Fig. 4B and C). However, only a minimal percentage of ASCs analyzed were considered dead (Fig. 4B and C). Even though the Foxp3 buffer set increased the percentage of dead BCs that were gated, this did not impact PE gMFIs as total and dead BCs showed similar PE background when stained with rIgG2a-PE (0.20 μg) (Fig. 4D). Overall, these data indicated that different fixation and permeabilization methods had little impact on the analysis of gated, viable ASCs.

Performance of one postfixation wash using the eBioscience Foxp3/transcription factor staining buffer set allows for robust intracellular staining of ASCs

The results discussed earlier indicated that a single postfixation wash protocol using either PFA + Sap or the Foxp3 buffer set may be suitable for ICFC of ASCs when PE-conjugated Abs are present. However, the Foxp3 buffer set, usually in the context of two postfixation washes, is believed to provide increased ICFC utility as it is designed to provide optimal staining of organelle-localized antigens including those in the nucleus [31]. To address these concepts, we compared the use of one or two postfixation washes with both buffer sets to detect Pro-IL-1β and TLR7 (Fig. 5A–E and Supplementary Fig. 4A–I).

Pro-IL-1β was chosen for the Immunological Genome Project (ImmGen, https://www.immgen.org) datasets have shown the *Il1b* gene to be preferentially expressed in SPL ASCs, particularly in PBs, when compared with total SPL BCs (Supplementary Fig. 4A). Pro-IL-1β has also been detected in protein lysates from human peripheral blood CD19$^+$ B cells [32]. Finally, cleavage of Pro-IL-1β to its mature IL-1β form and subsequent secretion typically requires the integration of multiple "danger" signals [33]. As a result, we hypothesized that Pro-IL-1β would accumulate and not be processed under homeostatic conditions thus facilitating its detection. TLR7 was selected as it predominantly localizes to the endosome [34] allowing for the comparison of cytoplasmic (i.e., Pro-IL-1β) versus organelle-localized protein staining efficacy. Additionally, *Tlr7* has been shown to be robustly expressed in mouse SPL BCs and ASCs (ImmGen, Supplementary Fig. 4B) as well as in human tonsillar counterparts [35].

For these experiments, we further gated SPL BCs as CD19$^+$ to confirm their identity (Supplementary Fig. 4C). Fixable live-dead staining was also included in all samples and only viable cells (i.e., negative for live-dead stain) were analyzed (Fig. 5A). The use of one postfixation wash (Fig. 5B) allowed for the detection of Pro-IL-1β in BCs as well as PBs and PCs for both buffer sets. In the context of PFA + Sap, Pro-IL-1β detection was significantly increased in PBs and PCs relative to BCs (Fig. 5D). Regardless of buffer set, two postfixation washes eliminated reliable detection of Pro-IL-1β in PBs and PCs due to retention of PE/Cy7 (Fig. 5Band D). This was demonstrated by the increased fluorescence signal of cells stained with rIgG1-PE/Cy7 isotype control (Fig. 5B and Supplementary Fig. 4E and F). Two washes also eliminated Pro-IL-1β detection in BCs; however, this was largely due to loss of signal when incubated with Abs directed at Pro-IL-1β (Fig. 5B and D and Supplementary Fig. 4D). The cause of this latter observation is unknown and may be an artifact resulting from cell processing as secretory lysosomes have been shown to house Pro-IL-1β in human monocytes [36]. Whether or not a similar phenomenon exists in BCs and if secretory lysosomes are lost in the cell preparation process used here requires further investigation.

Unlike Pro-IL-1β, TLR7 was minimally detectable when the 1 wash PFA + Sap protocol was utilized (Fig. 5C). Conversely, the one wash Foxp3 protocol resulted in the detection of TLR7 in BCs, PBs and PCs (Fig. 5C and E). PFA + Sap in combination with two postfixation washes showed intermediate TLR7 staining in BCs when compared with results observed with a single postfixation wash using PFA + Sap and Foxp3 buffers (Fig. 5B and D and Supplementary Fig. 4G). Respective to BCs, the two wash Foxp3 buffer protocol was equivalent to the one-wash version as both displayed ∼56–62% average TLR7 positivity (Fig. 5C and E). Examination of PBs and PCs demonstrated PE retention when two postfixation washes were used in the context of PFA + Sap (Fig. 5C and Supplementary Fig. 4H and I). We also observed PB and PC retention of PE in two postfixation wash Foxp3 buffer

set samples (Fig. 5C). Rather than an overall shift in gMFI, the retention observed resembled the previously mentioned "tail" pattern (Fig. 5C and Supplementary Fig. 4H and I) and resulted in an underestimation of the overall percentage of TLR7^{+} PBs and PCs (Fig. 5E). In general, both one postfixation wash protocols suppressed PE/Cy7 and PE retention by ASCs which allowed for detection of the protein targets shown here. However, the one postfixation wash Foxp3 buffer set protocol allowed for the detection of cytoplasmic as well as organelle-localized proteins.

DISCUSSION

While it has been reported that ASCs nonspecifically retain PE in the context of ICFC [25, 26], our current study confirms and extends these findings to include PE/Cy7. A key finding shown here is that the mere act of repetitive centrifugation postfixation appears to induce the ASC retention of PE. As such, a reduction in the number of postfixation centrifugation steps that occur before ICFC staining ameliorates this phenotype thus allowing for the utilization of extremely bright PE and PE/Cy7 fluorochromes in ASC ICFC.

Previous attempts [25, 26] to eliminate ASC retention of PE using multiple types of commercial ICFC buffer sets have been unsuccessful. These have included the BD Biosciences CytoFix/Cytoperm buffer set [25] as well as Foxp3 buffer sets from BD Biosciences, BioLegend and eBioscience/Thermo Fisher Scientific [26]. Standard protocols for these buffer sets call for multiple centrifugation steps following initial cellular fixation. The only exception to this is the eBioscience Foxp3 buffer set which provides multiple ICFC protocols. One of these, Protocol B, uses a single mandatory centrifugation step postfixation and was tested and shown to be "curative" in this study (Figs. 3 and 5). Single postfixation centrifugation was also sufficient to reduce PE retention in the context of PFA + Sap providing some flexibility in what buffers are utilized (Figs. 2 and 5). This may be an important consideration as different antigens display altered sensitivities regarding how fixation impacts their Ab-binding epitopes. In the context of the protein targets tested here, optimal staining of ASC intracellular proteins was observed while using the eBioscience Foxp3/Transcription Factor Staining Buffer Set rather than PFA + Sap (Fig. 5). This was most obvious when one postfixation centrifugation was performed (Fig. 5) and may simply be a result of the permeabilization agents that differ between buffers. Sap is a "weak" detergent that has been used to permeabilize fixed cells for ICFC; however, instances have been observed in which Sap does not effectively permeabilize certain types of membranes [37]. Under these circumstances, Triton X-100 has served as a more appropriate method as this "strong" detergent is commonly used for IF of nuclear proteins [38]. While the permeabilizing agent contained within the eBioscience Foxp3/Transcription Factor Staining Buffer Set used here is not explicitly stated, similar kits such as the Human FoxP3 Buffer Set (Catalog # 560098) from BD Biosciences are known to contain MeOH, a common reagent used to fix and permeabilize cells during ICFC [39]. Relatedly, we did observe differences in the type of PE retention when PFA + Sap and Foxp3 buffer sets were compared. We speculate that this may simply be a consequence of how the different buffer sets interact with cells. For example, PFA fixation leads to protein–protein crosslinks that also preserve overall cell structure. In contrast, MeOH is an organic solvent that precipitates proteins through dehydration resulting in distortion of cellular morphology. This is readily observed when forward and side scatter properties of cells treated with these reagents are examined on a flow cytometer. However, the idea remains to be tested. Lastly, we did find some variance between isotypes in the magnitude of PE and PE/Cy7 retention (Fig. 1). Previous studies have shown that unconjugated PE can be retained by ASCs in a concentration-dependent manner [25, 26]. As such, our observation referenced earlier may be related to differences in constant domain structure between Ab isotypes [40]. For example, differences in lysine amino acid number may directly impact the efficiency of fluorochrome conjugation [41]. In this sense, increased lysine residues within a particular isotype could lead to a higher ratio of fluorochrome conjugation and thus higher retention of PE.

An obvious question becomes why do ASCs exhibit PE retention and by extension, why does centrifugation augment this retention phenotype? While our study does not directly address this, a possibility may be related to the major function of ASCs which is the production of Abs. Of note, Abs are heavily glycosylated [42] and various compounds exist that bind carbohydrates [43] facilitating their detection independent of specific Ab–antigen interactions. Therefore, it is tempting to speculate that the high abundance of intracellular immunoglobulins combined with repetitive centrifugation can induce PE retention through incidental damage to cellular glycoproteins resulting in exposure to PE-interacting surfaces or structures. Alternatively, ASCs possess an expanded ER and Golgi network which could also suffer from the same postcentrifugation consequences hypothesized for Abs. Along these lines, it would be of interest to investigate PE retention in other cells which possess an expanded ER compartment such as pDCs [44]. Would the deletion of *Xbp1* which leads to loss of the expanded ER network in ASCs [45] and pDCs [46] result in the loss of PE retention?

Regardless of causation, the ability to ameliorate PE retention, as shown here, now facilitates the usage of PE- and PE/Cy7- conjugated Abs in assessing intracellular protein expression by ASCs. This is relevant to stand-alone analysis of ASCs as well as comparison to other cell types such as naive or activated BCs. This is a critical point as BC to ASC differentiation has been correlated with the acquisition of selected cytokine expression [23, 47] and could theoretically serve as a key diagnostic tool in the right context [48]. As such, reducing any potential for a false positive is critical [49]. To this end, FMOs and isotype control Abs have both been utilized in the field of flow cytometry and hotly debated regarding which strategy provides the "correct" analysis. We would suggest that much like anything else; this depends on context. For ICFC of ASCs, the use of PE- and PE/Cy7-conjugated isotype control Abs is critical in identifying a retention phenotype (Fig. 1) [25, 26]

that would have been misinterpreted for positive staining if only FMO samples and those stained with target-specific Abs were assessed.

Finally, we provide biological insight at the protein level into the evolution of ASCs and their potential to interact with the surrounding environment. RNA sequencing of mouse bone marrow PCs [50], as well as a quantitative polymerase chain reaction of human peripheral blood PBs and tonsillar PCs [35], has demonstrated expression of *Tlr7* at the gene level. We show here that a portion of SPL ASCs expresses TLR7 (Fig. 5). Given the role of this protein during viral responses [51], it will be interesting to see how ASC expression of TLR7 changes during infection and whether or not this contributes to the functionality of these cells. Furthermore, we showed relatively equivalent Pro-IL-1β expression in SPL PBs and PCs (Fig. 5). This contrasted RNA sequencing data available in the ImmGen database (http://rstats.immgen.org/Skyline/skyline.html) which illustrates enriched expression of *Il1b* transcripts in SPL PBs relative to PCs (Supplementary Fig. 4A). This may reflect active *Il1b* transcription and translation in PBs with Pro-IL1β protein being preloaded and maintained in PCs upon their subsequent maturation. This type of regulatory circuit has been previously defined within germinal center B cells as they transition between light and dark zone states [52]. Alternatively, these differences may be due to the use of varied gating strategies as PBs and PCs in the Immgen analysis were bifurcated based upon Prdm1-green fluorescent protein reporter activity as well as major histocompatibility complex class II expression.

In summary, we have identified a key contributing factor to the ASC retention of PE and its related molecules (i.e., PE/Cy7) during ICFC. It should be noted that this and other studies [25, 26] regarding ASC retention of PE have focused on mouse cells. Human ASCs are ultrastructurally similar to those of mice (e.g., expanded ER network); however, it is currently unknown if human ASCs suffer from the same PE retention. Regardless, we provide a framework to not only determine the existence of PE retention in human ASCs and other cell types (e.g., pDCs) but to also ameliorate its impact on ICFC staining.

DATA AVAILABILITY

The data underlying this article will be shared upon reasonable request to the corresponding author.

AUTHORS' CONTRIBUTIONS

K.A.T.P. and P.D.P. conceptualized the study. P.R., M.C., M.K., and K.A.T.P. performed experiments. K.A.T.P. and P.D.P. analyzed the data. P.D.P. wrote the manuscript and all authors approved the final version.

ACKNOWLEDGEMENTS

Flow cytometry was performed at the WMed Flow Cytometry and Imaging Core which is managed by Michael Clemente.

CONFLICT OF INTEREST STATEMENT

The authors declare no commercial or financial relationships that could be construed as a potential conflict of interest.

FUNDING

This study was supported by startup funds from the Western Michigan University Homer Stryker M.D. School of Medicine.

ETHICS AND CONSENT

Not applicable.

ANIMAL RESEARCH

All experiments were performed with the approval of the WMed Institutional Animal Care and Use Committee (IACUC). Care was taken throughout the study to prevent any undue animal suffering.

REFERENCES

1. Amanna, IJ, Carlson, NE, Slifka, MK. Duration of humoral immunity to common viral and vaccine antigens. *N Engl J Med* 2007; **357**: 1903–15.
2. Fairfax, KA, Kallies, A, Nutt, SL *et al.* Plasma cell development: from B-cell subsets to long-term survival niches. *Semin Immunol* 2008; **20**: 49–58.
3. Gaudette, BT, Allman, D. Biochemical coordination of plasma cell genesis. *Immunol Rev* 2021; **303**: 52–61.
4. Manakkat Vijay, GK, Singh, H. Cell fate dynamics and genomic programming of plasma cell precursors. *Immunol Rev* 2021; **303**: 62–71.
5. Nutt, SL, Hodgkin, PD, Tarlinton, DM *et al.* The generation of antibody-secreting plasma cells. *Nat Rev Immunol* 2015; **15**: 160–71.
6. Landsverk, OJ, Snir, O, Casado, RB *et al.* Antibody-secreting plasma cells persist for decades in human intestine. *J Exp Med* 2017; **214**: 309–17.
7. Manz, RA, Lohning, M, Cassese, G *et al.* Survival of long-lived plasma cells is independent of antigen. *Int Immunol* 1998; **10**: 1703–11.
8. Slifka, MK, Antia, R, Whitmire, JK *et al.* Humoral immunity due to long-lived plasma cells. *Immunity* 1998; **8**: 363–72.
9. Ma, K, Wang, X, Shi, X *et al.* The expanding functional diversity of plasma cells in immunity and inflammation. *Cell Mol Immunol* 2020; **17**: 421–2.
10. McGettigan, SE, Debes, GF. Immunoregulation by antibody secreting cells in inflammation, infection, and cancer. *Immunol Rev* 2021; **303**: 103–18.
11. Pioli, PD. Plasma cells, the next generation: beyond antibody secretion. *Front Immunol* 2019; **10**: 2768.
12. Shaffer, AL, Shapiro-Shelef, M, Iwakoshi, NN *et al.* XBP1, downstream of Blimp-1, expands the secretory apparatus and other organelles, and increases protein synthesis in plasma cell differentiation. *Immunity* 2004; **21**: 81–93.
13. Zhu, H, Bhatt, B, Sivaprakasam, S *et al.* Ufbp1 promotes plasma cell development and ER expansion by modulating distinct branches of UPR. *Nat Commun* 2019; **10**: 1084.
14. Matsumoto, M, Baba, A, Yokota, T *et al.* Interleukin-10-producing plasmablasts exert regulatory function in autoimmune inflammation. *Immunity* 2014; **41**: 1040–51.
15. Rojas, OL, Probstel, AK, Porfilio, EA *et al.* Recirculating intestinal IgA-producing cells regulate Neuroinflammation via IL-10. *Cell* 2019; **177**: 492–3.

16. Chavele, KM, Merry, E, Ehrenstein, MR. Cutting edge: circulating plasmablasts induce the differentiation of human T follicular helper cells via IL-6 production. *J Immunol* 2015; **194**: 2482–5.
17. Chin, SS, Chorro, L, Chan, J *et al.* Splenic innate B1 B cell Plasmablasts produce sustained granulocyte-macrophage Colony-stimulating factor and Interleukin-3 cytokines during murine malaria infections. *Infect Immun* 2019; **87**: e00482–19.
18. Rauch, PJ, Chudnovskiy, A, Robbins, CS *et al.* Innate response activator B cells protect against microbial sepsis. *Science* 2012; **335**: 597–601.
19. Weber, GF, Chousterman, BG, Hilgendorf, I *et al.* Pleural innate response activator B cells protect against pneumonia via a GM-CSF-IgM axis. *J Exp Med* 2014; **211**: 1243–56.
20. Lino, AC, Dang, VD, Lampropoulou, V *et al.* LAG-3 inhibitory receptor expression identifies immunosuppressive natural regulatory plasma cells. *Immunity* 2018; **49**: 120, e129–33.
21. Meng, L, Almeida, LN, Clauder, AK *et al.* Bone marrow plasma cells modulate local myeloid-lineage differentiation via IL-10. *Front Immunol* 2019; **10**: 1183.
22. Shen, P, Roch, T, Lampropoulou, V *et al.* IL-35-producing B cells are critical regulators of immunity during autoimmune and infectious diseases. *Nature* 2014; **507**: 366–70.
23. Suzuki-Yamazaki, N, Yanobu-Takanashi, R, Okamura, T *et al.* IL-10 production in murine IgM(+) CD138(hi) cells is driven by Blimp-1 and downregulated in class-switched cells. *Eur J Immunol* 2017; **47**: 493–503.
24. Batard, P, Szollosi, J, Luescher, I *et al.* Use of phycoerythrin and allophycocyanin for fluorescence resonance energy transfer analyzed by flow cytometry: advantages and limitations. *Cytometry* 2002; **48**: 97–105.
25. Kim, MS, Kim, TS. R-phycoerythrin-conjugated antibodies are inappropriate for intracellular staining of murine plasma cells. *J Int Soc Anal Cytol* 2013; **83**: 452–60.
26. Bohacova, P, Kossl, J, Hajkova, M *et al.* Difference between mitogen-stimulated B and T cells in nonspecific binding of R-phycoerythrin-conjugated antibodies. *J Immunol Methods* 2021; **493**: 113013.
27. Matsuda, Y, Fujii, T, Suzuki, T *et al.* Comparison of fixation methods for preservation of morphology, RNAs, and proteins from paraffin-embedded human cancer cell-implanted mouse models. *J Histochem Cytochem* 2011; **59**: 68–75.
28. Ribatti, D. The discovery of plasma cells: an historical note. *Immunol Lett* 2017; **188**: 64–7.
29. Katkov, II, Mazur, P. Factors affecting yield and survival of cells when suspensions are subjected to centrifugation. Influence of centrifugal acceleration, time of centrifugation, and length of the suspension column in quasi-homogeneous centrifugal fields. *Cell Biochem Biophys* 1999; **31**: 231–45.
30. Kim, IH, Yang, JD, Lee, DG *et al.* Evaluation of centrifugation technique and effect of epinephrine on fat cell viability in autologous fat injection. *Aesthet Surg J* 2009; **29**: 35–9.
31. Law, JP, Hirschkorn, DF, Owen, RE *et al.* The importance of Foxp3 antibody and fixation/permeabilization buffer combinations in identifying CD4+CD25+Foxp3+ regulatory T cells. *J Int Soc Anal Cytol* 2009; **75**: 1040–50.
32. Lim, KH, Chen, LC, Hsu, K *et al.* BAFF-driven NLRP3 inflammasome activation in B cells. *Cell Death Dis* 2020; **11**: 820.
33. Gurung, P, Li, B, Subbarao Malireddi, RK *et al.* Chronic TLR stimulation controls NLRP3 inflammasome activation through IL-10 mediated regulation of NLRP3 expression and Caspase-8 activation. *Sci Rep* 2015; **5**: 14488.
34. Kuznik, A, Bencina, M, Svajger, U *et al.* Mechanism of endosomal TLR inhibition by antimalarial drugs and imidazoquinolines. *J Immunol* 2011; **186**: 4794–804.
35. Dorner, M, Brandt, S, Tinguely, M *et al.* Plasma cell toll-like receptor (TLR) expression differs from that of B cells, and plasma cell TLR triggering enhances immunoglobulin production. *Immunology* 2009; **128**: 573–9.
36. Andrei, C, Margiocco, P, Poggi, A *et al.* Phospholipases C and A2 control lysosome-mediated IL-1 beta secretion: implications for inflammatory processes. *Proc Natl Acad Sci U S A* 2004; **101**: 9745–50.
37. Mercanti, V, Cosson, P. Resistance of Dictyostelium discoideum membranes to saponin permeabilization. *BMC Res Notes* 2010; **3**: 120.
38. Spector, DL. Immunofluorescence localization of nuclear proteins. *Cold Spring Harb Protoc* 2011; **2011**: 1276–80.
39. Levitt, D, King, M. Methanol fixation permits flow cytometric analysis of immunofluorescent stained intracellular antigens. *J Immunol Methods* 1987; **96**: 233–7.
40. Schroeder, HW Jr, Cavacini, L. Structure and function of immunoglobulins. *J Allergy Clin Immunol* 2010; **125**: S41–52.
41. Nanna, AR, Li, X, Walseng, E *et al.* Harnessing a catalytic lysine residue for the one-step preparation of homogeneous antibody-drug conjugates. *Nat Commun* 2017; **8**: 1112.
42. Irvine, EB, Alter, G. Understanding the role of antibody glycosylation through the lens of severe viral and bacterial diseases. *Glycobiology* 2020; **30**: 241–53.
43. Sun, X, Zhai, W, Fossey, JS *et al.* Boronic acids for fluorescence imaging of carbohydrates. *Chem Commun (Camb)* 2016; **52**: 3456–69.
44. Colonna, M, Trinchieri, G, Liu, YJ. Plasmacytoid dendritic cells in immunity. *Nat Immunol* 2004; **5**: 1219–26.
45. Taubenheim, N, Tarlinton, DM, Crawford, S *et al.* High rate of antibody secretion is not integral to plasma cell differentiation as revealed by XBP-1 deficiency. *J Immunol* 2012; **189**: 3328–38.
46. Iwakoshi, NN, Pypaert, M, Glimcher, LH. The transcription factor XBP-1 is essential for the development and survival of dendritic cells. *J Exp Med* 2007; **204**: 2267–75.
47. Shi, W, Liao, Y, Willis, SN *et al.* Transcriptional profiling of mouse B cell terminal differentiation defines a signature for antibody-secreting plasma cells. *Nat Immunol* 2015; **16**: 663–73.
48. Fink, K. Origin and function of circulating Plasmablasts during acute viral infections. *Front Immunol* 2012; **3**: 78.
49. Savasan, S, Buck, S, Gadgeel, M *et al.* Flow cytometric false myeloperoxidase-positive childhood B-lineage acute lymphoblastic leukemia. *Cytometry B Clin Cytom* 2018; **94**: 477–83.
50. Pioli, PD, Casero, D, Montecino-Rodriguez, E *et al.* Plasma cells are obligate effectors of enhanced Myelopoiesis in aging bone marrow. *Immunity* 2019; 351–66.e6.
51. Lester, SN, Li, K. Toll-like receptors in antiviral innate immunity. *J Mol Biol* 2014; **426**: 1246–64.
52. Kennedy, DE, Okoreeh, MK, Maienschein-Cline, M *et al.* Novel specialized cell state and spatial compartments within the germinal center. *Nat Immunol* 2020; **21**: 660–70.